

RSC Advances



This is an *Accepted Manuscript*, which has been through the Royal Society of Chemistry peer review process and has been accepted for publication.

Accepted Manuscripts are published online shortly after acceptance, before technical editing, formatting and proof reading. Using this free service, authors can make their results available to the community, in citable form, before we publish the edited article. This *Accepted Manuscript* will be replaced by the edited, formatted and paginated article as soon as this is available.

You can find more information about *Accepted Manuscripts* in the [Information for Authors](#).

Please note that technical editing may introduce minor changes to the text and/or graphics, which may alter content. The journal's standard [Terms & Conditions](#) and the [Ethical guidelines](#) still apply. In no event shall the Royal Society of Chemistry be held responsible for any errors or omissions in this *Accepted Manuscript* or any consequences arising from the use of any information it contains.

One pot synthesis of doxorubicin loaded gold nanoparticles for sustained drug release

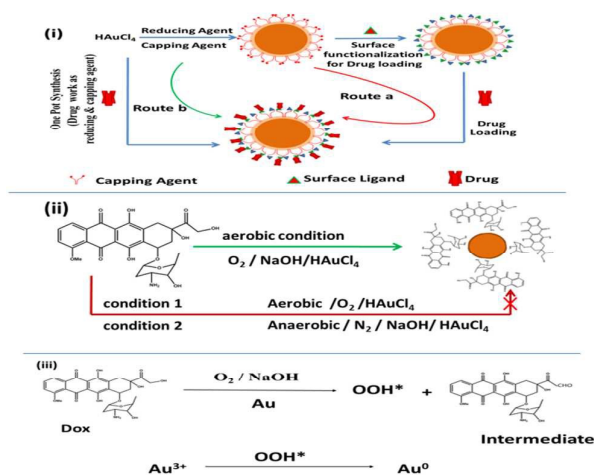
Received 00th January 20xx,
Accepted 00th January 20xx

Abhishek Chaudhary, Charu Dwivedi, Abhishek Gupta, Chayan K Nandi*

Abstract: Here, we report a facile, versatile and simple one-pot synthesis of doxorubicin (Dox) loaded gold nanoparticles (Dox-GNP conjugate), where Dox can act both as reducing as well as capping agent. Interestingly, when the conjugate was placed into the transporter protein environment, it avoided the undesirable multilayer protein corona formation, which is very common for nanomaterials. The *in vitro* drug release kinetic studies and the cytotoxicity assay and cellular uptake efficiency advocates that the system is capable of sustained release of the drug even in the presence of complex biological environment.

The therapeutic efficiency of any chemotherapeutic drug largely depends upon its bioavailability at a particular site, which relies on its design and fabrication. Various reports are available in the literature proving that in contrast to the free drug molecules, the pharmacokinetics and therapeutic index of the drugs is significantly improved. This can be achieved by loading drugs onto the surface of nanostructures such as metal nanoparticles, polymeric nanoparticles and liposomes, through the physical encapsulation, surface adsorption or chemical conjugation.¹ Especially, gold nanoparticles (GNP) have emerged as attractive candidate for delivering various payloads into their targets due to its proven biocompatibility and low cytotoxicity.^{2,3} Additional advantage of GNP is the ease of their surface functionalization, which can enhance the efficacy of the drug delivery by reducing the uptake by the reticuloendothelial system and preventing nonspecific binding to biological substances.^{4,5} Doxorubicin, an anthracycline anti-tumor drug when administered directly, lacks tumor-targeting ability which leads to poor therapeutic efficacy and severe side effects including cardio toxicity and myelosuppression.⁶ Another disadvantage of administering the bare Dox molecule is the development of chemo resistance due to the over expression of a membrane transporter, p-glycoprotein, that actively pumps Dox out of the cell.⁷ Oppositely, Dox conjugated nanoparticles based drug delivery system is taken up by the cells efficiently through endocytosis and can minimize chemo resistance and ill effects towards normal cells.⁸ The unearthing of this fact has motivated

significant research on nanoparticles assisted drug delivery system. General strategies for linking drug to nanoparticles involves multi steps including the synthesis of nanoparticles, surface functionalization by bio-compatible functional groups and followed by incorporation of drug (as shown in Scheme i, route a). However, most of the processes are complicated and even involve harsh chemical intermediates which can cause unwanted cell death.⁹ Herein, we are presenting a facile and unique one-pot route for loading of Dox onto the GNP and its sustained release. In the synthesis process, Dox acts as both reducing agent for synthesizing GNP as well as capping agent for GNP stabilization. The schematic of the synthesis of Dox-GNP conjugate is furnished in Scheme i (route b). The synthesis of Dox-GNP conjugate is carried out by reacting optimized concentrations of HAuCl₄ (0.25 mM / 5 ml) with Dox (10 μM / 5 ml) under basic condition (pH 10) with moderate stirring (Figure S1a and b, Supporting Information). An optimum temperature of 50°C is chosen for carrying out of the reaction (Figure S2, Supporting Information).



Scheme i: Schematic representation of generally adapted multistep process (route a) and the proposed single step one pot synthesis (route b) of Dox-GNP conjugated nanoparticles. **Scheme ii:** Schematic representation of the Dox-GNP conjugate synthesis under different reaction condition. **Scheme iii:** Mechanism of Dox-GNP conjugate synthesis where O₂ can abstract the proton from –CH₂OH group of Dox and thus forming aldehyde and OOH* as intermediates. Finally, OOH* species helped in reducing the Au³⁺ to Au⁰ in alkaline solution

School of Basic Sciences, Indian Institute of Technology Mandi, Himachal Pradesh, 175001, India

Electronic Supplementary Information (ESI) available: [details of any supplementary information available should be included here]. See DOI: 10.1039/x0xx00000x

The absorption spectra of bare Dox (Fig. 1a) shows one band centered at 490 nm associated with the π - π^* transition and a shoulder at around 360 nm attributed to partially forbidden n - π^* transitions involving the three C=O group.^{6,10} These characteristic bands of free Dox molecule are disappeared and an absorption band pertaining to the surface plasmon resonance (SPR) of GNP starts appearing at 525 nm on completion of reaction (3 h). The progress of the reaction is also evident from the change in the color of the reaction mixture from pale yellow to purple. (Inset Fig. 1a). No further change in the absorption band at 525 nm (A_{525}) is observed indicating the completion of the reaction (Fig. 1b). The average size of the synthesized particles is 25 nm as determined by TEM analysis (Fig. 1c) and DLS (Dynamic light scattering) measurement (Figure S3, Supporting Information). The zeta potential of Dox-GNP conjugate was found to be -32 mV, which confirms the stability of synthesized nanoparticle conjugate. The reduction of Au^{3+} to Au^0 proceeds through catalytic oxidation of alkyl alcoholic group of Dox in alkaline condition with molecular oxygen in the presence of gold as catalyst.^{11,12} O_2 can abstract the hydrogen atom of the -OH group from alcohol to yield OOH^* species and aldehyde as an intermediate.¹³ Paclawski and Fitzner have reported that OOH^* species (generated from $[Au(OH)_4]^-$ & $[HO_2]^-$) can reduce the complex gold (III) ions to metallic gold in alkaline solution (Scheme iii).¹⁴ To verify this hypothesis, the similar reaction is carried out under nitrogen atmosphere (Scheme ii). Even after 24 h of reaction time, formation of GNP could not be realized proving the necessity of O_2 in the process (Figure S4a and 4b, Supporting Information). The role of NaOH in the reaction progress is further investigated, and, it is observed that the absence of NaOH from the reaction mixture obstructed the synthesis of nanoparticles. NaOH is quintessential in the synthesis of gold nanoparticles, as it furnishes the hydroxyl group in aqueous environment which accelerates the reduction of Au^{3+} to Au^0 . However, in the absence of Dox, only NaOH is not able to reduce Au^{3+} to Au^0 (Figure S5, Supporting Information and schematic ii) Modification of the -NH₂ group of the glycosidic ring of Dox into -NH(C₂H₅) also produced GNP (Figure S6, Supporting Information), confirming that the terminal -CH₂OH group is mainly responsible for the reduction process of Au^{3+} to Au^0 and leaving anthraquinone ring of the drug (responsible for drug activity) unchanged.¹⁵ The stability of anthraquinone ring is further confirmed by the HRMS analysis of pure Dox, and Dox released from Dox-GNP conjugated system. The mass peak at 397 corresponding to anthraquinone ring of Dox released from the synthesized drug matches well with that of the pure Dox molecule (Figure S7, Supporting Information). These results indicate that the effective part of the antitumor drug remains unaffected during the synthesis process. Capping of the synthesized GNP with Dox molecule is also evident from the emission spectra of the synthesized system. The free Dox shows fluorescence emission maximum at 594 nm with an excitation source at 480 nm, whereas, fluorescence is completely quenched on its conjugation with GNP. This result confirms the surface adsorption of drug on GNP (Fig. 1d), where the surface energy transfer (SET) leads to quenching off fluorescence of free Dox.¹⁶ At this stage, it is necessary to check the stability of the Dox-GNP conjugate in different pH and salt solution. The possible particle agglomeration in the complex biological environment might result in undesirable accumulation in some organs, and trigger chronic immune responses. The synthesized conjugate is found to be stable upto 20 mM of NaCl and microscopic coagulation starts appearing at 30 mM of NaCl concentration (Figure S8a, Supporting Information.). It is observed that the synthesized Dox-GNP

conjugate is more stable as compared to the most commonly used citrate coated GNP (Figure S8b, Supporting Information.). The synthesized system is also quite stable in the pH range 5 to 12, but at lower pH (pH<4) the nanoparticles tend to lose their stability (Figure S9, Supporting Information). The observed red shift of 60 nm and the 8 % decrease in the absorption intensity at pH=2 could be due to nanoparticles coagulation. It is reported that the protein corona and its dynamic behavior may effectively hinder the chemical and surface properties of the designed nanoparticles and alter the specificity in targeting,¹⁷ bio-distribution, and cytotoxicity thus leading to nano-biotherapeutic failures.¹⁸ On the other hand, this nonspecific protein corona formation could also be exploited to tune the release of drug molecule from nanoparticles carriers in addition to loading and performing triggered release of the drug molecules.¹⁹ Therefore, it's imperative to inspect the interaction of the developed system with serum protein. We have systematically investigated the interaction of Dox-GNP conjugate with human serum albumin (HSA) by monitoring the changes in the hydrodynamic size of the nanoparticles. It is observed that hydrodynamic size of nanoparticles increased only by 12 nm as a result of protein nanoparticles interaction (Fig. 2a). A red shift of 6 nm in the SPR band of the Dox-GNP conjugate upon equilibration for 2 h with HSA also supports the increase in the hydrodynamic size observed in the DLS measurements (Figure S10, Supporting Information).

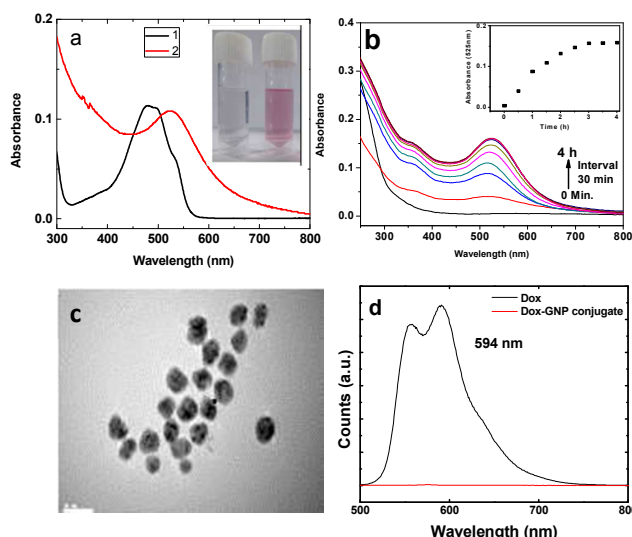


Fig. 1: (a) UV-vis Spectra of Dox (curve 1) and Dox-GNP (Curve 2), (b) Kinetics of Dox-GNP conjugate formation monitored by the absorption spectra after regular time interval of 30 minutes (inset shows Dox-GNP synthesis by recording surface plasmon at 525 nm) (c) TEM image of Dox-GNP conjugate and (d) Steady state fluorescence of Dox and Dox-GNP conjugate showed a complete quenching of fluorescence in the conjugated system.

On contrary, the citrate coated GNP (without DOX conjugation), under similar condition, showed multi-layered protein adsorption with around ~60 nm increment in their hydrodynamic diameter (inset Fig. 2a). The secondary structure of HSA was unperturbed by the Dox-GNP conjugate as evident from circular dichroism spectroscopy (Figure S11, Supporting Information). The practical applicability of the synthesized system is investigated by monitoring the in-vitro release of Dox and the cell viability assay in the cancer cell line. The data is compared with the free Dox molecule. It is

observed that $\sim 80\%$ of free Dox is released in first 2 h, whereas the synthesized conjugate system showed sustained release of bound Dox in 10 mM PBS buffer of pH 7.4, 6.6 and 5.0. The release pattern of conjugated system showed an initial burst for first 10 h, and then a sustained release followed up to 72 h.

The loosely bound drug might release fast at the initial stage followed by its sustained release. The cumulative release of Dox (%) from Dox-GNP conjugates at pH 7.4, 6.6 and 5.0 is almost similar which could be of additional advantage for drug delivery, as the system is indifferent to the acidic extracellular and intracellular environments of tumors (Fig. 2b). However, the drug release at pH 5.0 is comparatively higher for initial 20 h. This could be due to the protonation of the GNP surface bound $-\text{NH}_2$ group of Dox at lower pH and hence release of drug from the GNP surface.

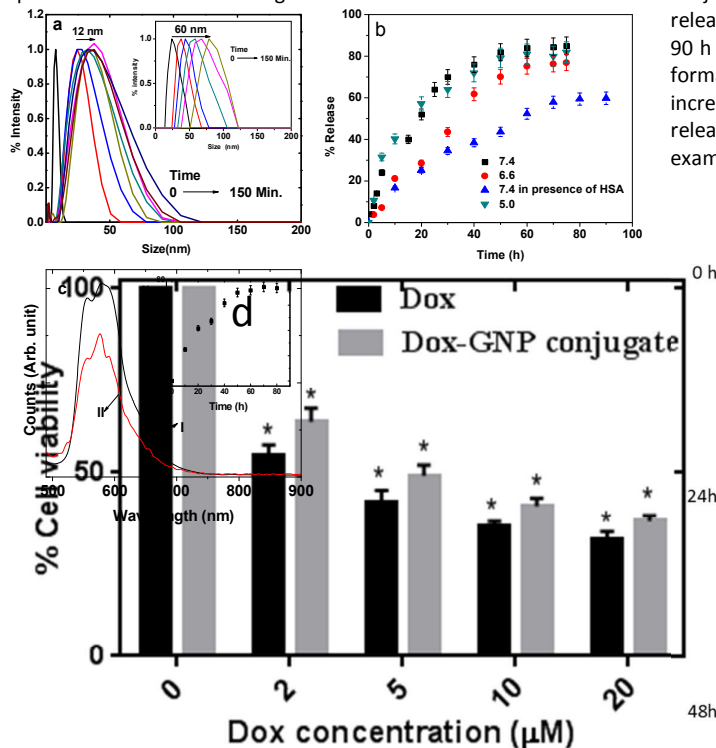
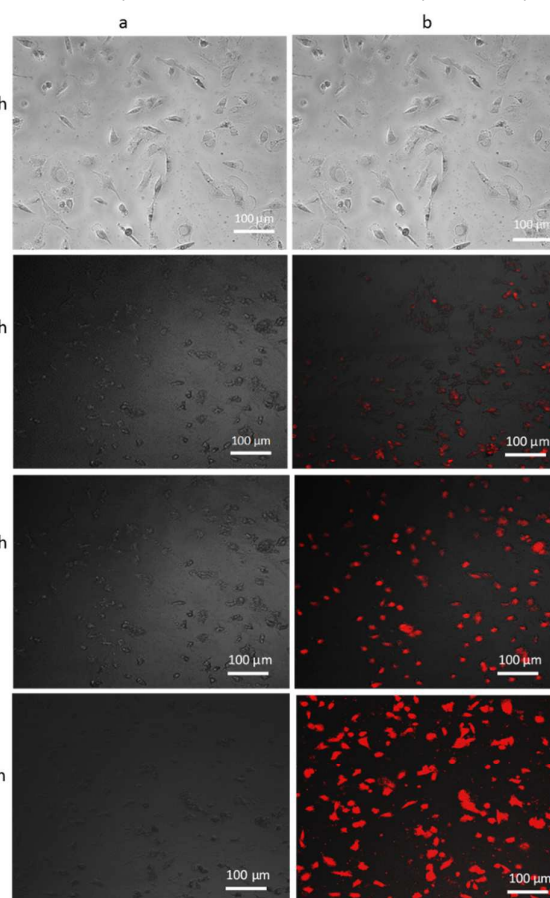


Fig. 2: Time dependent kinetics of the protein corona formation (a) around the synthesized Dox-GNP conjugate, and inset a, around the citrate coated GNP (b) Time dependent study of the percentage release of Dox from the surface of the synthesized Dox-GNP conjugated nanoparticles at 7.4 and 6.6 and in the presence of HSA at pH 7.4 (c) GNP fluorescence spectra of free Dox used during dialysis (curve I) and Dox released from Dox-GNP conjugate after 80 h of dialysis (curve II), (inset c) fluorescence recovery from Dox-GNP conjugate by dialysis method at every 10 h interval and (d) cell viability of MDA-MB-231 cells after treatment with free Dox and Dox-GNP conjugate at varying concentration, Dox and Dox-GNP conjugate were incubated with cells for 72 h at 37°C . Value shows the mean \pm SD of two independent experiments. Treated groups showed statistically significant differences from the control group by the Student's t-test (* $P < 0.05$)

Around 70 % fluorescence recovery was also observed after 80 h of dialysis (Fig. 2c). This result also supports the observation that SET is mainly responsible for fluorescence quenching of Dox. The release

of fluorescent drug molecule can be used in tracking the path of released drug in bio imaging studies without using any additional fluorophores. Various reports are available on different release profile of Dox from nano-biotherapeutic agents such as multifunctional hybrid silica nanoparticles (80%, 25 h),²⁰ PEG-GNP (80%, 48 h),⁷ PEG-Dox system²¹ (20%, 80 h), etc. It is evident from the literature that even after multistep functionalization of nanoparticles, efficient and sustained release of the drug is hard to accomplish.

Some reports show that the cumulative release and the sustained release behavior of Dox is further compromised in the complex biological medium.²² Therefore, the in-vitro release (at physiological pH) of the bound drug in presence of HSA protein (HSA-Dox-GNP conjugate) is also checked. As shown in Fig. 2b, the cumulative release of Dox from the HSA-Dox-GNP conjugate system is $\sim 57\%$ in 90 h at room temperature. This result suggests that the monolayer formation of HSA protein around Dox-GNP conjugate system increases the residence time of the drug and insures sustained release. Further, the antitumor efficacy of the Dox-GNP conjugate is examined by MTT (3-(4,5-dimethylthiazol-2-yl)-2,5-



diphenyltetrazolium bromide) colorimetric assay using breast cancer cell line (MDA-MB-231). The viability of the cells after exposure to free Dox and Dox-GNP conjugate for 24, 48 and 72 h is depicted in Figure S12, Supporting Information. It is evident from the results, that about 40 % of cells are alive after being treated with free Dox for 24 h. In contrast, the viability of the cells is 48 % even after 72 h of treatment with Dox-GNP conjugate. These results indicate that the bioavailability of Dox is increased upto 72 h in the case of Dox-GNP conjugate.

Fig.3: Confocal images of MDA-MB-231 cells when incubated with Dox-GNP conjugate for 0 h, 24 h, 48 h, and 72 h at 37 °C (a = cell under bright field, b = cell merge image).

The concentration causing death of 50 % cell (IC_{50} value) is also determined for free drug and the Dox-GNP conjugates against MDA-MB 231, in a dose dependent manner. The IC_{50} values for Dox and Dox-GNP conjugate are found to be 2.23 and 5.65 μ M, respectively (Fig. 2d & S12b).). Finally the cellular uptake efficiency and intracellular distribution of Dox-GNP conjugates have been monitored in MDA-MB-231 cells. To this endeavor, the cells were incubated with Dox-GNP conjugate for 24, 48 and 72 h, respectively. The confocal images in Fig. 3 show that with increasing the incubation time, the uptake efficiency of the released drug from the conjugate is increased. For example, the number of fluorescent spots and as well as the intensity is maximum after 72 h of incubation, while no fluorescence was observed at 0 h of incubation.²⁴ These results suggests that the loaded Dox can be released efficiently inside the cells and the released Dox has maintained its activity during the synthesis process. However, the activity of the Dox-GNP conjugate is lower as compared to the free Dox. This could be due to the difference in the uptake mechanism of the pure drug from that of the conjugated drug system. The Dox-GNP conjugates are internalized by the cell through endocytosis followed by endo-lysosomal escape and subsequent drug distribution in the cytosol and nucleus.²⁴⁻²⁶ While free Dox is internalized by passive diffusion, which is very fast process as compared to endocytosis process.¹⁰ This slow release of the drug from the nanoparticle conjugate could be of extra advantages as it increases the bioavailability of drug, for improving the cell cytotoxicity.

Conclusions

In brief, this study reports a new, simple one pot synthesis of Dox-GNP conjugates which can be used for drug delivery without further processing. The terminal $-CH_2OH$ group of Dox takes part in GNP formation under basic conditions. The synthesized nanoparticles are quite stable under physiological pH and have better stability than that of the widely studied citrate capped GNP. The excellent drug release profile and the cell viability viability and cellular uptake efficiency data shows that the synthesized conjugates hold good potential for use as an efficient drug delivery system even in the complex biological matrix.

Corresponding Author

*E-mail: chayan@iitmandi.ac.in. Tel.:+91 1905237917. Fax: +91 1905 237942

Acknowledgments

The authors acknowledge home institute, Indian Institute of Technology Mandi (IIT Mandi) and Department of science & Technology India (Project SR/FT/CS-152/2011) and Department of Biotechnology India (BT/PR4067/BRB/10/1128/2012) for all the financial support. Advanced Material Research Centre Facilities of IIT Mandi is also being acknowledged.

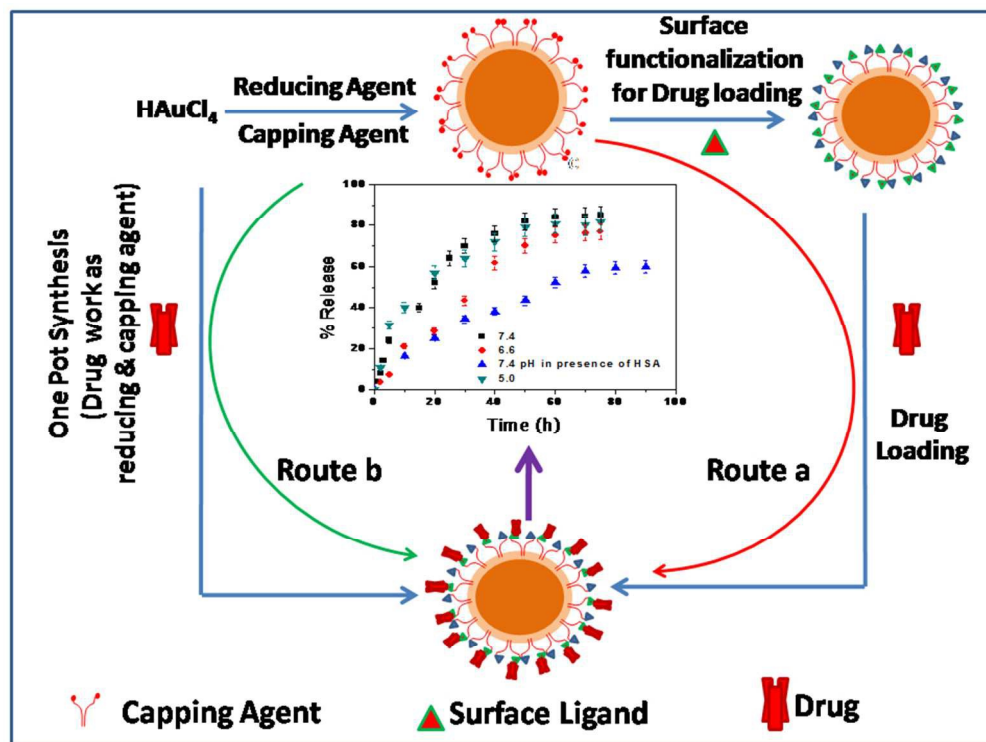
References

1. L. Zhang, D. Pornpattananangkul, C. M. J. Hu and C. M. Huang, *Curr. Med. Chem.*, 2010, **17**, 585.
2. C. M. Alexander, M. M. Maye and J. C. Dabrowiak, *Chem. Commun.*, 2011, **47**, 3418.
3. R. Venkatesan, A. K. Pichaimani, K. Hari, P. K. Balasubramanian, J. Kulandaivel and K. Premkumar, *J. Mater. Chem. B*, 2013, **1**, 1010.
4. J. Mieszawska, W. J. M. Mulder, Z. A. Fayad and D. P. Cormode, *Mol. Pharmaceutics*, 2013, **10**, 831.
5. R. Hong, G. Han, J. M. Fernandez, B. J. Kim, N. S. Forbes and V. M. Rotello, *J. Am. Chem. Soc.*, 2006, **128**, 1078.
6. P. C. Barret, T. Gustavsson, D. Markovitsi, I. Manet and S. Monti, *Phys. Chem. Chem. Phys.*, 2013, **15**, 2937.
7. F. Wang, Y. C. Wang, S. Dou, M. H. Xiong, T. M. Sun and J. Wang, *ACS Nano*, 2011, **5**, 3679.
8. M. Prabakaran, J. J. Grailer, S. Pilla, D. A. Steeber and S. Gong, *Biomaterial*, 2009, **30**, 6065.
9. S. J. Soenen, B. Manshian, M. J. Montenegro, F. Amin, B. Meermann, T. Thiron, M. Comelissen, F. Vanhaecke, S. Doak, W. J. Parak, S. D. Smedt and K. Braeckmans, *ACS Nano*, 2012, **6**, 5767.
10. L. G. Smulevich and M. P. Marzocchi, *Spectrochimica acta*, 1982, **38**, 213.
11. B. N. Zope, D. D. Hibbitts, M. Neurock and R. J. Davis, *Science*, 2010, **330**, 74.
12. J. Guzman and B. C. Gates, *J. Am. Chem. Soc.*, 2004, **126**, 2672.
13. C. R. Chang, X. F. Yang, B. Long and J. Li, *ACS Catal.*, 2013, **3**, 1693.
14. K. Paclawski and K. Fitzner, *Metall. Mater. Trans. B*, 2006, **37B**, 703.
15. Morgan, Lee, Roy, *European patent application*: EP 0300100.
16. H. Tao, X. Liao, M. Xu, X. Xie, F. Zhong and Z. Sheng, *Anal. Methods*, 2014, **6**, 2560.
17. A. Chaudhary, A. Gupta, S. Khan and C. K. Nandi, *Phys. Chem. Chem. Phys.*, 2014, **16**, 20471.
18. V. Mirshafiee, M. Mahmoudi, K. L. J. Chengd and M. L. Kraft, *Chem. Commun.*, 2013, **49**, 2557.
19. L. B. Berdón, D. Pozzi, G. Caracciolo, A. L. Capriotti, G. Caruso, C. Cavaliere, Riccioli, A. S. Palchetti and A. Laganà. *Langmuir*, 2013, **29**, 6485.
20. X. Hu, X. Hao, Y. Wu, J. Zhang, X. Zhang, P. C. Wang, G. Zou and X. J. Liang, *J. Mater. Chem. B*, 2013, **1**, 1109.
21. P. Gou, W. Liu, W. Mao, J. Tang, Y. Shen and M. Su, *J. Mater. Chem. B*, 2013, **1**, 284.
22. L. Tang, R. Tong, V. J. Coyle, Q. Yin, H. Pondenis, L. B. Borst, J. Cheng and T. M. Fan, *ACS Nano.*, 2015, **9**, 5072.
23. J. Wang, P. P. Gao, X. X. Yang, T. T. Wang, J. Wang and C. Z. Huang, *J. Mater. Chem. B* 2014, **2**, 4379.
24. S. Khan, A. Gupta and C. K. Nandi, *J. Phys. Chem. Lett.*, 2013, **4**, 3747.
25. M. R. K. Ali, S. I. R. Panikkanvalappil and M. A. El Sayed, *J. Am. Chem. Soc.*, 2014, **136**, 4464.

Journal Name

COMMUNICATION

26. B. J. Kim, H. Cheong, B. H. Hwang and H. J. Cha, *Angew. Chem. Int. Ed.*, 2015, **54**, 7318.



254x190mm (96 x 96 DPI)